

## Parvovirus B19-Infected Tubulointerstitial Nephritis in Hereditary Spherocytosis

Kei Nishiyama,<sup>1</sup> Yuka Watanabe,<sup>1</sup> Masataka Ishimura,<sup>1</sup> Kenichi Tetsuhara,<sup>2</sup> Takashi Imai,<sup>1</sup> Hikaru Kanemasa,<sup>1</sup> Kenji Ueki,<sup>3</sup> Yoshitomo Motomura,<sup>1</sup> Noriyuki Kaku,<sup>2</sup> Yasunari Sakai,<sup>1</sup> Ken-Ichi Imadome,<sup>1</sup> and Shouichi Ohga<sup>1</sup>

<sup>1</sup>Department of Pediatrics, Graduate School of Medical Sciences, Kyushu University, Fukuoka, Japan, <sup>2</sup>Pediatric Intensive Care Unit, Kyushu University Hospital, Fukuoka, Japan, <sup>3</sup>Department of Medicine and Clinical Science, Graduate School of Medical Sciences, Kyushu University, Fukuoka, Japan, <sup>4</sup>Department of Advanced Medicine for Infections, National Center for Child Health and Development, Tokyo, Japan

**Background.** Human parvovirus B19 (B19V) causes glomerulopathy or microangiopathy, but not tubulopathy. We experienced an 11-year-old girl with spherocytosis who developed acute kidney injury on a primary infection of B19V. She presented with anuria, encephalopathy, thrombocytopenia, and coagulopathy, along with no apparent aplastic crisis.

**Methods.** Continuous hemodiafiltration, immunoglobulin, and intensive therapies led to a cure.

**Results.** A kidney biopsy resulted in a histopathological diagnosis of tubulointerstitial nephritis without immune deposits. The virus capsid protein was limitedly expressed in the tubular epithelial cells with infiltrating CD8-positive cells.

**Conclusions.** Viral and histopathological analyses first demonstrated B19-infected tubulointerstitial nephritis due to the aberrant viremia with hereditary spherocytosis.

**Keywords.** parvovirus B19; spherocytosis; tubulointerstitial nephritis.

Parvovirus B19 (B19V) is a nonenveloped virus with a diameter of 23–26 nm that contains a linear single-stranded deoxyribonucleic acid (DNA) genome of 5.6 kb, flanked by 2 identical terminal hairpin structures [1]. This small virus, originally isolated from the screening panels of hepatitis B virus, is classified as an *Erythroparvovirus* of the *Parvoviridae* family. Parvovirus B19 infects only susceptible humans, and the protective immunity persists for the lifetime of person. Primary infection of B19V causes erythema infectiosum, transient cytopenias in

children, and nonimmune hydrops fetalis in pregnant women [2]. Subclinical infection occurs in approximately 30% of children and 60% of adults. If affected individuals have hemolytic or immunodeficiency diseases, severe complications occur during the primary infection or reactivation, including aplastic crisis, hemophagocytic lymphohistiocytosis (HLH), cardiomyopathy, encephalopathy, arthropathy, liver failure, and bone marrow failure. However, fatal B19V disease in otherwise healthy subjects has been unexplained.

Parvovirus B19 exhibits high tropism for erythroid progenitor cells (EPCs) in the bone marrow and fetal liver. Restricted replication of the virus in erythroid lineage cells accounts (1) for the expression of receptor and coreceptor(s) on the cell surface of human EPCs and (2) for the intracellular factors essential for virus replication [3]. Parvovirus B19 DNA persists lifelong in various tissues of the tonsils, testicles, kidneys, muscle, salivary glands, thyroid, skin, liver, heart, brain, bone marrow, and bone [4]. Parvovirus B19 infection precipitates rheumatic diseases, although little is known about the effect of B19V DNA on specific cell types. This virus causes acute glomerulopathy or microangiopathy but have not been reported about interstitial nephritis [5, 6].

In this study, we report an 11-year-old girl with hereditary spherocytosis who developed acute renal failure, encephalopathy, thrombocytopenia, and coagulopathy during primary infection of B19V. For the first time, a renal biopsy defined the entity of B19V-infected tubulointerstitial nephritis.

### CASE PRESENTATION

An 11-year-old Japanese girl with spherocytosis visited our hospital because of a 1-day fever and oliguria. She complained of headache, abdominal pain, and vomiting. Because of seizure and cardiopulmonary arrest just after admission, this patient entered pediatric intensive care. Her father and grandfather had hereditary spherocytosis. She received the diagnosis of spherocytosis at 10 months old but lived an active life with borderline anemia.

On admission, her consciousness level was Glasgow coma scale E1V1M3 on respiratory support. The body temperature was 39.8°C, pulse rate was 144 beats/minute, and blood pressure was 149/75 mmHg. Physical examinations revealed jaundice, sluggish dilated pupils, splenomegaly, and edema. Complete blood counts showed  $13.0 \times 10^9/L$  neutrophil dominant leukocytosis, a hemoglobin concentration of 10.3 g/dL, hematocrit 29.2%, reticulocytes 75%, and a platelet count of  $92.0 \times 10^9/L$ . A prolonged prothrombin time (42.3 seconds; reference range [rr], 10.0–13.5) and activated partial thromboplastin time (120.6 seconds; rr, 26.0–41.0) as well as decreased fibrinogen (106 mg/dL; rr, 150–300) and increased

Received 10 June 2020; editorial decision 1 July 2020; accepted 2 July 2020.

Correspondence: Kei Nishiyama, MD, Department of Pediatrics, Graduate School of Medical Sciences, Kyushu University, 3-1-1 Maidashi, Higashi-ku, Fukuoka 812-8582, Japan (nkei@pediatr.med.kyushu-u.ac.jp).

#### Open Forum Infectious Diseases®

© The Author(s) 2020. Published by Oxford University Press on behalf of Infectious Diseases Society of America. This is an Open Access article distributed under the terms of the Creative Commons Attribution-NonCommercial-NoDerivs licence (<http://creativecommons.org/licenses/by-nc-nd/4.0/>), which permits non-commercial reproduction and distribution of the work, in any medium, provided the original work is not altered or transformed in any way, and that the work is properly cited. For commercial re-use, please contact journals.permissions@oup.com  
DOI: 10.1093/ofid/ofaa288

fibrin/fibrinogen degradation product levels (791.4  $\mu\text{g}/\text{mL}$ ; rr,  $<5.0 \mu\text{g}/\text{mL}$ ) indicated consumption coagulopathy. Peripheral blood smears showed spherocytosis but no schizocytes. Blood chemistries revealed increased levels of creatinine 4.03 mg/dL (rr, 0.35–0.58), blood urea nitrogen 74 mg/dL (rr, 8–20), total bilirubin 3.1 mg/dL (rr, 0.3–1.2), aspartate aminotransferase 478 U/L (rr, 12–30), alanine aminotransferase 148 U/L (rr, 3–18), and lactic dehydrogenase 2255 U/L (rr, 150–231). C-reactive protein concentration was 9.91 mg/dL (rr,  $<0.06$ ). The serum complement levels were decreased: C3 63 mg/dL (rr, 65–135), C4 13 mg/dL (rr, 13–40), and CH50 17.7 U/mL (rr, 25–48). Urinalyses showed hemoglobinuria and proteinuria (3.9 g/g creatinine) but not hematuria or casts. Urine  $\beta_2$ -microglobulin was 76 310  $\mu\text{g}/\text{L}$  (rr,  $<300 \mu\text{g}/\text{L}$ ). No causative bacteria were isolated from the blood or stool cultures. Plasma ADAMTS13 activity was  $<1\%$  (rr,  $>10\%$ ), and ADAMTS13 inhibitor was negative (cutoff  $<0.4$  Bethesda titer). Serum B19V-specific immunoglobulin (Ig)M and IgG antibodies were undetectable. Serum B19V DNA was  $>10^{11}$  copies/mL (cutoff  $10^2$ ). A cerebrospinal fluid study was unremarkable. Hyperferritinemia (29 839 ng/mL; rr, 10–80) and hypercytokinemia (soluble interleukin-2 receptor 3981 U/mL, rr = 145–519; and interleukin-6 4156.7 pg/mL, rr = 0.447–9.96) indicated macrophage activation syndrome (MAS). Flow cytometric analyses of peripheral blood indicated no T-cell activation. Magnetic resonance imaging revealed mild brain edema. Electroencephalography

showed high-voltage slow waves. Despite normal echocardiography findings, pulmonary bleeding occurred on ventilator support.

Continuous renal replacement therapy (CRRT) and plasma therapy were started for the control of acute kidney injury (AKI) and coagulopathy (Figure 1). Under a tentative diagnosis of B19V-driven thrombotic thrombocytopenic purpura (TTP), intravenous Ig, high-dose steroid therapy, and plasma exchange (PE) and/or infusions were started. During 6 courses of PE, she regained full consciousness with subdural hematoma. A restored activity of ADAMTS13 and no abnormal multimers of von Willebrand factor indicated consumption coagulopathy.

She was then weaned from CRRT and assist ventilation. She was discharged from the hospital without hematuria or proteinuria on day 47 of admission. Serum creatinine levels were normalized. Urine  $\beta_2$ -microglobulin decreased to  $<100 \mu\text{g}/\text{L}$ . Serum B19V DNA decreased to  $10^2$  copies/mL, and the virus-specific antibody titers showed seroconversion. She returned to an active school life with mild brain atrophy. Three months later, the Wechsler Intelligence Scale for Children (4th ed.) revealed a borderline IQ of 75 with impaired perceptual reasoning, working memory, and processing speed.

#### Ethical Statement

This study was approved by the local ethics committee, and written informed consent was obtained from patient and her parents.

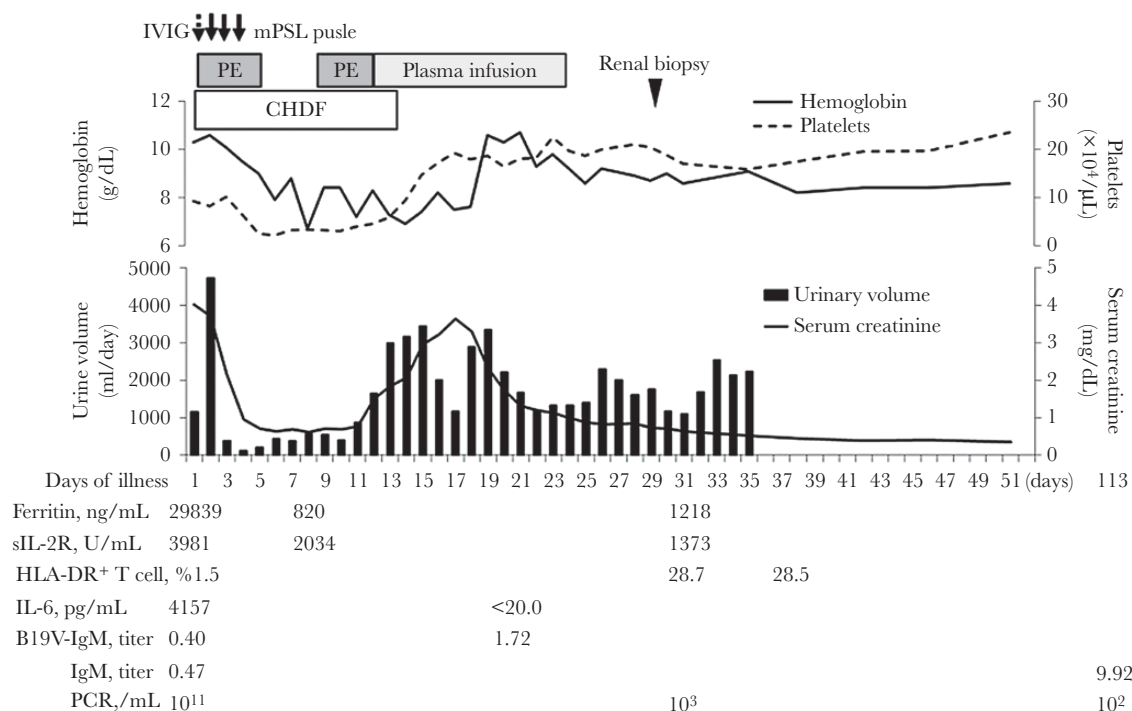


**Figure 1.** Clinical course of the present case. B19V, parvovirus B19; CHDF, continuous hemodiafiltration; HLA-DR, human leucocyte antigen D-related; Ig, immunoglobulin; IL, interleukin; IVIG, intravenous immunoglobulin; mPSL, methylprednisolone; PCR, polymerase chain reaction; PE, plasma exchange; sIL-2R, soluble interleukin-2 receptor.

## METHODS

Renal tissue was obtained by percutaneous renal biopsy in the patient. The specimens were studied by light microscopy (LM) and immunofluorescence (IF). For LM, a portion of the kidney biopsy was fixed in periodate-lysine-paraformaldehyde, embedded in paraffin, cut at 3  $\mu$ m, and treated with hematoxylin and eosin, periodic acid-Schiff, and periodic acid silver methenamine. For IF, kidney fragments were embedded in OCT compound, snapfrozen in *n*-hexane cooled with a mixture of dry ice and acetone, and cut at 5  $\mu$ m and stained with antihuman IgG, IgA, IgM, C3, C1q, and fibrinogen.

Paraffin-embedded renal biopsy sections were also analyzed for B19V-specific viral capsid proteins, CD8, CD56, and CD20 by immunohistochemistry. Heat-induced epitope retrieval was performed using microwave for 15 minutes in antigen retrieval buffer (pH9; Nichirei, Tokyo, Japan). After washing with Tris-buffered saline (TBS), one of the following primary antibodies was applied: mouse anti-parvovirus B19 monoclonal antibody (1:200; Chemicon, no. MAB8293), rabbit antihuman CD8 monoclonal antibody (1:500; Abcam, no. ab93278), mouse antihuman CD56 monoclonal antibody (1:100; Invitrogen, no. 07-5603), and mouse antihuman CD20 (1:5; Nichirei, no. 422741). After incubating overnight at 4°C, sections were washed in TBS 3 times and incubated with peroxidase-labeled antirabbit or antimouse antibody (Histofine Simplestain Max PO; Nichirei) for 30 minutes at room temperature. Peroxidase activity was detected with diaminobenzidine ([DAB] Sigma-Aldrich). Sections were counterstained with hematoxylin and dehydrated.

Flow cytometry was performed using a cell analyzer (Sony, no. EC800). Multicolor staining was carried out using phycoerythrin-, Brilliant Violet 711-, Brilliant Violet 421-, phycoerythrin-cyanin5-, or phycoerythrin-cyanin7-conjugated monoclonal antibodies against, CD3, CD4, CD8, CD14, and CD19 (Beckman Coulter or BioLegend). Mononuclear cells (MNCs) were separated from peripheral blood using Vacutainer CPT (BD, no. 362753) and were then fractionated into CD3<sup>-</sup>CD19<sup>+</sup>, CD3<sup>+</sup>CD4<sup>+</sup>, CD3<sup>+</sup>CD8<sup>+</sup>, and CD3<sup>-</sup>CD19<sup>-</sup>CD14<sup>+</sup> cells, in >98% of purity, using a cell sorter (Sony, no. SH800Z). Real-time polymerase chain reaction (PCR) was performed in the laboratory of BML Inc. (Tokyo, Japan). Deoxyribonucleic acid was isolated from sorted cells (CD4<sup>+</sup>, CD8<sup>+</sup>, CD14<sup>+</sup>, and CD19<sup>+</sup> cells) and frozen renal tissue using the QIAamp DNA Mini Kit (QIAGEN, no. 51304). The presence of B19V DNA was assessed by real-time PCR, using the following: forward primer, 5'-TGC AGTATTATCTAGTGAAGACTTACACAA-3'; reverse primer, 5'-ATGAATCCTTGCAGCACTGTC-3'; probe, 5'-FAM-CTGGGCAAGTTAGCGTACAACCTACCCGGTA-TAMRA-3'.

## RESULTS

On day 29 of admission, LM of kidney biopsy samples revealed tubulointerstitial nephritis with lymphocyte infiltration (Figure 2A–C). No glomerular or vascular lesion was found. There were no immunofluorescence-positive deposits for IgG, IgA, IgM, C3, or C1q. Tubular epithelial cells were exclusively positive for the monoclonal antibody against the epitope of VP1 and VP2 (Figure 2D–F). The B19 capsid protein was stained in the proximal tubules and also to lesser extent in the distal tubules. Tubular inflammation was confined to the proximal tubules (Figure 2D). The infiltrating cells were positive for CD8 and CD56 but not CD20 (Figure 2G–I). The kidney biopsy sample contained a high copy number of B19V DNA ( $3.2 \times 10^6$  copies/ $\mu$ g DNA). When the viral load was assessed in sorted subpopulations of peripheral blood MNCs, CD3<sup>-</sup>CD19<sup>+</sup> cells contained B19V DNA ( $1.4 \times 10^4$  copies/ $\mu$ g DNA), but CD3<sup>+</sup>CD4<sup>+</sup>, CD3<sup>+</sup>CD8<sup>+</sup>, or CD3<sup>-</sup>CD19<sup>-</sup>CD14<sup>+</sup> cells had no detectable virus DNA.

## DISCUSSION

This is the first report of B19V-associated acute tubulointerstitial nephritis. The virus capsid protein was notably expressed in the tubular epithelium of B19V DNA-loaded kidney. Infiltrating cells were CD8<sup>+</sup> T-cells harboring no B19V DNA. The aggressive AKI was considered to have arisen from the ectopic infection and inflammation with hyperviremia.

Severe complications occur in acute B19V infection. At the first presentation of TTP-like disease, no red cell fragmentations were found. Stable circulation did not augment the renal damage after resuscitation. This case met the diagnostic criteria of MAS/HLH leading to kidney inflammation. We summarized 19 reported patients with B19V-associated MAS/HLH, including our own (Supplementary Table 1). Fifteen (76%) had hemolytic anemia or immunodeficiency leading to hyperviremia. The most frequently involved organs were the liver, heart, central nervous system (CNS), and kidney, in that order. All 5 patients (patients 1, 7, 8, 10, and 15) survived AKI, and 4 (21%) died from 3 CNS disease or 1 myocarditis. This suggests a message that AKI occurs in cases of B19V-driven MAS/HLH but can fully improve after intensive therapy.

The pathophysiology of B19V-associated AKI is a major concern. Parvovirus B19 causes immune complex-mediated glomerulonephritis as the most common form of AKI. Thirty-two cases of B19V-associated renal complication have been reported, including the present one (Supplementary Table 2). Endocapillary or mesangial proliferative glomerulonephritis occurred in 25 patients (78%). They had a prodrome phase (3 days–2 months) until the renal manifestation, detectable B19V-specific IgM or IgG antibody titers, and immune deposits in the kidney tissues. Anti-B19V antibodies produce circulating immune complexes and subsequent deposits in the mesangial

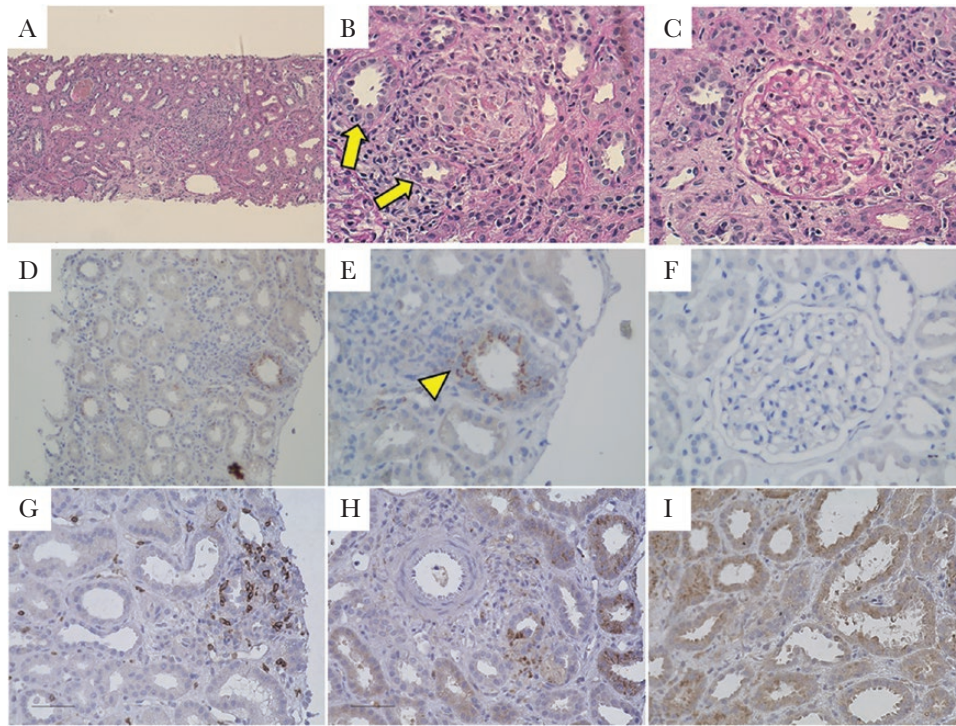


**Figure 2.** Light microscopic findings of the kidney biopsy samples. (a and b) Mononuclear cells infiltrate into the edematous interstitial areas. There are several foci of clustering inflammatory cells (arrows) around the tubular epithelium (Periodic-acid Schiff [PAS] staining; original magnification  $\times 100$  [a],  $\times 400$  [b]). (c) Glomeruli showed minimal abnormality. The glomerular capillaries are patent, with neither thickening nor irregularity of the capillary wall (PAS staining, original magnification  $\times 400$ ). (d and e) B19 capsid protein-positive tubular cells (arrow head) are scattered around the area of mononuclear cell infiltration (immunohistochemical [IHC] staining of B19 capsid antigen; original magnification  $\times 100$  [d],  $\times 400$  [e]). (f) Note that glomeruli do not show B19 capsid protein positivity (IHC staining of B19 capsid protein; original magnification  $\times 400$ ). (e–i) CD8- or CD56-positive cells are found among the infiltrating mononuclear cells, but not CD20-positive cells (IHC staining of CD8 [g], CD56 [h], and CD20 [i], respectively; original magnification  $\times 400$ ).

or subendothelial spaces, provoking acute endocapillary proliferative glomerulonephritis [7]. However, in our case, AKI abruptly occurred at the peak viremia without detectable B19V antibodies or immune deposits. High viral loads in hemolytic diseases including hereditary spherocytosis, or immunological diseases, are associated with more severe B19V disease [8]. Productive B19V infection is restricted to human EPCs, particularly at the stage of burst-forming unit-erythroid to colony-forming unit-erythroid. Erythropoietin and hypoxia also play a critical role for the efficient replication. In this line, severe reversible AKI might occur in association with hyperinflammation and hyperviremia. Regarding the pathogenesis of AKI, there might be some factors other than tubulointerstitial nephritis. In the present case, serum creatinine levels had been already elevated at the time of cardiac arrest, suggesting that acute tubular necrosis after cardiac arrest was not the leading cause of AKI. However, the renal histology did not determine the effect size of tubulointerstitial nephritis or acute tubular necrosis on AKI. In this setting, the resuscitation might have contributed to the exacerbation of AKI.

The cellular tropism of B19V remains unclear. In a reported case of B19V-associated collapsing glomerulopathy, the capsid antigen was positive for podocytes, parietal epithelial cells, and

tubular epithelial cells [9]. In contrast, it showed limited expression in the tubular epithelial cells of our case. Parvovirus B19 infects cells through the main receptor, P-antigen, and 2 coreceptors ( $\alpha_5\beta_1$  integrin and Ku80) [10]. P-antigen, a receptor for P-fimbriated *Escherichia coli*, is the predominant glycolipid of the human kidney and uroepithelial cells. However, these do not express  $\alpha_5\beta_1$  integrin or Ku80. Parvovirus B19 capsid binds P-antigen and undergoes a conformational change, exposing VP1u, which is required for internalization [11]. Therefore, B19V might have internalized tubular epithelial cells via adhesion to P-antigen after VP1u exposure. In a recent study, nephrotropic parvovirus has been reported to cause chronic tubulointerstitial nephritis in rodents, although the tropism for the tubular epithelial cells remains elusive [12]. The sequence homology between the present strain of B19V and mouse nephrotropic parvovirus was not studied because the virus genome was not isolated in our patient.

## CONCLUSIONS

Parvovirus B19 DNA persists lifelong in human tissues, but little is known about the fate of specific cell types harboring B19V. Long-lived memory B cells are reservoir candidates for B19V,

where no virus replication was demonstrated [13]. Antibody-dependent enhancement is a mechanism of B19V entry into monocytes and endothelial cells. However, undetectable B19V-specific IgG and absent Ig deposits did not support the antibody-dependent mechanism of infection in our patient. In this context, the presence of virus capsid antigen in tubular cells indicates ectopic infection rather than replication. We demonstrated a novel AKI due to B19V-infected tubulointerstitial nephritis arising from hyperviremia in hemolytic disease.

### Supplementary Data

Supplementary materials are available at *Open Forum Infectious Diseases online*. Consisting of data provided by the authors to benefit the reader, the posted materials are not copyedited and are the sole responsibility of the authors, so questions or comments should be addressed to the corresponding author.

### Acknowledgments

We thank Dr. Tamami Tanaka (Department of Pediatrics, Graduate School of Medical Sciences, Kyushu University) for performing the cell sorting using flow cytometry, Katsuhiko Miki (Advanced Technology and Developmental Division, BML, Inc.) for performing polymerase chain reaction for parvovirus B19 deoxyribonucleic acid, Mikio Munakata (Department of Medicine and Clinical Science, Graduate School of Medical Sciences, Kyushu University) for technical assistance, and Drs. Etsuro Nanishi and Yuuki Iwaya (Department of Pediatrics, Graduate School of Medical Sciences, Kyushu University) for treatment and helpful discussion, along with all of the staff who treated the patients in Kyushu University Hospital.

**Author contributions.** K. N., T. I., M. I., and S. O. were the principal investigators, taking primary responsibility for the paper. K. N. and S. O. wrote the manuscript. Y. W., K. T., H. K., Y. M., N. K., and Y. S. performed the clinical management with helpful discussion regarding the completion of the work. K. U. and K.-I. I. conducted the histopathological analysis and gave advice on the quality control of viral studies, respectively.

**Disclaimer.** The funder had no role in study design, data collection and analysis, decision to publish, or preparation of the manuscript.

**Financial support.** This study was funded by the Morinaga Foundation for Health and Nutrition.

**Potential conflicts of interest.** All authors: No reported conflicts of interest. All authors have submitted the ICMJE Form for Disclosure of Potential Conflicts of Interest.

### References

1. Cossart YE, Field AM, Cant B, Widdows D. Parvovirus-like particles in human sera. *Lancet* **1975**; 1:72–3.
2. Cotmore SF, Agbandje-McKenna M, Chiorini JA, et al. The family *Parvoviridae*. *Arch Virol* **2014**; 159:1239–47.
3. Leisi R, von Nordheim M, Kempf C, Ros C. Specific targeting of proerythroblasts and erythroleukemic cells by the VP1u region of parvovirus B19. *Bioconjug Chem* **2015**; 26:1923–30.
4. Servant-Delmas A, Morinet F. Update of the human parvovirus B19 biology. *Transfus Clin Biol* **2016**; 23:5–12.
5. Watanabe T. Renal involvement in human parvovirus B19 infection. *Pediatr Nephrol* **2003**; 18:966–7.
6. Ardalan MR, Shoja MM, Tubbs RS, et al. Postrenal transplant hemophagocytic lymphohistiocytosis and thrombotic microangiopathy associated with parvovirus b19 infection. *Am J Transplant* **2008**; 8:1340–4.
7. Ieiri N, Hotta O, Taguma Y. Characteristics of acute glomerulonephritis associated with human parvovirus B19 infection. *Clin Nephrol* **2005**; 64:249–57.
8. Sim JY, Chang LY, Chen JM, et al. Human parvovirus B19 infection in patients with or without underlying diseases. *J Microbiol Immunol Infect* **2019**; 52:534–41.
9. Besse W, Mansour S, Jatwani K, et al. Collapsing glomerulopathy in a young woman with APOL1 risk alleles following acute parvovirus B19 infection: a case report investigation. *BMC Nephrol* **2016**; 17:125.
10. Munakata Y, Saito-Ito T, Kumura-Ishii K, et al. Ku80 autoantigen as a cellular coreceptor for human parvovirus B19 infection. *Blood* **2005**; 106:3449–56.
11. Bönsch C, Zuercher C, Lieby P, et al. The globoside receptor triggers structural changes in the B19 virus capsid that facilitate virus internalization. *J Virol* **2010**; 84:11737–46.
12. Roediger B, Lee Q, Tikoo S, et al. An atypical parvovirus drives chronic tubulointerstitial nephropathy and kidney fibrosis. *Cell* **2018**; 175:530–543.e24.
13. Pyöriä L, Toppinen M, Mäntylä E, et al. Extinct type of human parvovirus B19 persists in tonsillar B cells. *Nat Commun* **2017**; 8:14930.